www.czasopisma.pan.pl PAN POLSKA AKADEMIA NAUK www.journals.pan.pl

archives
of thermodynamics
Vol. **40**(2019), No. 1, 49–69
10.24425/ather.2019.128289

Triple diffusive flow of Casson nanofluid with buoyancy forces and nonlinear thermal radiation over a horizontal plate

MANJAPPA ARCHANA [a]
BIJJANAL JAYANNA GIREESHA [a]
BALLAJJA CHANDRAPPA PRASANNAKUMARA[*b]

[a] Department of Studies and Research in Mathematics, Kuvempu University, Shankaraghatta-577451, Shimoga, Karnataka, India

[b] Government First Grade College, Koppa, Chikkamagaluru-577126, Karnataka, India

Abstract The presence of more than one solute diffused in fluid mixtures is very often requested for discussing the natural phenomena such as transportation of contaminants, underground water, acid rain and so on. In the paper, the effect of nonlinear thermal radiation on triple diffusive convective boundary layer flow of Casson nanofluid along a horizontal plate is theoretically investigated. Similarity transformations are utilized to reduce the governing partial differential equations into a set of nonlinear ordinary differential equations. The reduced equations are numerically solved using Runge-Kutta-Fehlberg fourth-fifth order method along with shooting technique. The impact of several existing physical parameters on velocity, temperature, solutal and nanofluid concentration profiles are analyzed through graphs and tables in detail. It is found that, modified Dufour parameter and Dufour solutal Lewis number enhances the temperature and solutal concentration profiles respectively.

Keywords: Triple diffusion; Casson nanofluid; Nonlinear thermal radiation; Buoyancy force

[*]Corresponding Author. Email: dr.bcprasanna@gmail.com

www.czasopisma.pan.pl PAN POLSKA AKADEMIA NAUK www.journals.pan.pl

Nomenclature

c_p	–	specific heat coefficient of nanoparticles
c_s	–	specific heat coefficient of fluid
C	–	concentration
D_B	–	Brownian diffusion coefficient
D_{CT}	–	soret type diffiusivity
D_S	–	solutal diffiusivity
D_T	–	thermophoretic diffusion coefficient
f	–	dimensionless velocity components
g	–	gravitational accelaration
q_r	–	radiative heat flux
Pr	–	Prandtl number
Ra_a	–	local Rayleigh number
u, v	–	velocity components
x, y	–	Cartesian coordinates

Greek symbols

α	–	thermal diffusivity of the fluid
β	–	casson fluid parameter
η	–	similarity variable
θ	–	dimensionless fluid temperature
$theta_w$	–	temperature ratio parameter
μ	–	coefficient of fluid viscosity
σ	–	Stefan-Boltzmann constant
τ	–	ratio of effective heat capacity of the nanoparticle material to heat capacity of the fluid
ϕ	–	dimensionless nanoparticle volume fraction
χ	–	dimensionless solute concentration
ψ	–	stream function

Subscripts

w	–	conditions at the wall
∞	–	free stream condition

1 Introduction

Triple diffusive convection is a natural phenomenon which can be seen in solidification of molten alloys, geothermally heated lakes, sea water and so on. It is a mixing process in which the density depends on three stratifying agencies such as heat and salts concentration having different diffusivities. When temperature and two or more component agencies are present then the physical and mathematical situation becomes increasingly richer. Griffiths extended the stability analysis of double diffusive convection flow by including the third diffusing component and he obtained that smaller dif-

www.czasopisma.pan.pl PAN POLSKA AKADEMIA NAUK www.journals.pan.pl

fusivity of third component has significant role on the nature of diffusive instabilities [1]. Kuznetsov and Nield have analytically explained the double diffusive convective flow of a nanofluid over a vertical plate [2]. Triple convective-diffusive fluid salted mixture over a horizontal layer was studied by Rionero [3]. Shivkumara and Naveen employed modified perturbation technique to analyse the nonlinear stability of a triple diffusive convection of Couple stress fluid [4]. Khan *et al.* compared triple diffusive fluid mixture with double diffusive mixture in boundary layer flow and found that for assisting flow rate of heat and mass transfer is higher but opposite for opposing flow [5]. Ghalambaz *et al.* have theoretically analysed the fluid flow in a porous medium consisting of two dissolved pollutants and they found that buoyancy ratio parameter increases the rate of heat and mass transfer at the wall [6].

In the field of advancement of nanotechnology, nanofluid is one of the best outcome for its fascinating thermophysical properties and was introduced by Choi [7]. The thermal performance of nanomaterials is much higher than the base fluids. Hence, it is quite necessary to combine these materials for the production of advanced heat transport liquid model which has high conductivity of methods. We can find its applications in many fields such as aerodynamic extrusion of plastic sheets, applied thermal engineering, structure and characterization of polymers, properties of polymers, compounding and processing of polymers and description of major polymers, petrochemical industry and so on. Meanwhile, interesting investigations on nanofluid flow and heat transfer can be seen in [8–12]. Moreover, some of the researchers have examined the triple diffusive convection in nanofluid flow. Rana *et al.* have incorporated the Buongiorno model to analyze the triple diffusive convection flow of nanofluid [13]. Goyal and Bhargava have considered the binary fluid flow over a nonlinear stretching sheet suspended with solute and Al_2O_3 nanoparticles in the presence of magnetic field [14]. They found that, magnetic effect increases the thickness of the thermal, solutal and nano-mass volume fraction. Khan *et al.* discussed the triple diffusive boundary layer flow of nanofluid along a horizontal and vertical plate subjected to the convective boundary condition [15,16].

The model of Newtonian fluid can be utilized to describe the flow characteristics of many materials by using a single constitutive equation. But, flow aspect of most of the materials that we encounter in our daily life exhibits the characteristics of non-Newtonian fluids and the properties of

www.czasopisma.pan.pl PAN POLSKA AKADEMIA NAUK www.journals.pan.pl

these fluids can't be explained by a single constitutive equation as that of in the case of Newtonian fluid. Significance of these types of fluids can be found in many industry and technology such as crude oil extraction from petroleum products, processing of food stuffs, production of paper, fiber coating, bioengineering and so on. Among many non-Newtonian fluids one of the fluids called Casson fluid behaves like elastic solid which is based on the yield shear stress. The model of this type of fluid was first introduced by Casson to anticipate the flow behavior of pigment-oil suspensions [17]. Many of the investigators are working on non-Newtonian fluids and some of the recent investigations that were undertaken by researchers are in [18–24].

As most of the scientific processes such as cooling of glass sheet, astrophysical flows, space vehicle re-entry and working of many advanced energy convection systems occur at high temperature in which nonlinear thermal radiation effect start to play a superficial role and cannot be neglected. The emission from hot walls and working fluid result in the form of thermal radiation. Thus, knowledge of radiation and its influence in heat transfer is essential. Makinde and Animasaun have reported the impact of nonlinear thermal radiation and quartic chemical reaction in nanofluid flow along a horizontal surface [25]. In the analysis carried out by Mustafa *et al.*, they obtained S shaped temperature profile for the temperature ratio parameter which signifies the case of adiabatic [26]. Archana *et al.* have stated the impact of nonlinear thermal radiation in three dimensional flow of Maxwell fluid suspended with nanoparticles in the presence of mass flux boundary conditions [27]. Further, this flow problem was extended by Ramesh *et al.* by incorporating the convective condition at the boundary along with porous effect [28]. Hussain *et al.* illustrated the effects of linear and nonlinear Rosseland thermal radiation through graphical representation in which they accomplished that temperature of the flow is dominated by the presence of nonlinear Rosseland thermal radiation [29]. Some more recent studies on nonlinear thermal radiation can be seen in [30,31].

As nanofluid with non-Newtonian modelling has become influential in view of its various applications, the principal aim of this investigation is to study the triple diffusive convective boundary layer flow of a Casson fluid along a horizontal plate suspended with nanoparticles. Further, triple diffusive convective boundary layer flow of non-Newtonian nanofluid in the presence of nonlinear thermal radiation has not yet been studied. Buongiorno's model is assimilated to study the effect of Brownian motion and

www.czasopisma.pan.pl PAN POLSKA AKADEMIA NAUK www.journals.pan.pl

thermophoretic force. The numerical solution is retrieved using Runge-Kutta-Fehlberg fourth-fifth order method along with shooting technique for the existing problem. Effects of several dimensionless parameters have been described through the graphical representation in detail.

2 Mathematical analysis

Consider a steady, laminar boundary layer free convection flow of an incompressible Casson nanofluid past the upward face of a horizontal flat plate saturated with two different salts having different properties. It is assumed that the mixture of nanofluid and salts is homogeneous and is in local thermal equilibrium. Also, Oberbecke-Boussinesq approximation is employed. In addition, the thermal energy equation includes regular diffusion and cross-diffusion terms for both components of salts having concentration, C_1 and C_2. Let T_w, C_w, C_{1w}, and C_{2w} be the constant values of the temperature, nanoparticle and solutal concentration of salt 1 and 2 of the plate, respectively, and these constant values are assumed to be larger than the ambient temperature, solutal concentrations and nanoparticle concentration, which are represented by T_∞, $C_{1\infty}$, $C_{2\infty}$, and C_∞, respectively. With the aforesaid assumptions, governing basic equations for the present flow representing conservation of mass, momentum, thermal energy, solute 1, solute 2 and nanoparticle concentrations are as follows:

$$\frac{\partial u}{\partial x} + \frac{\partial v}{\partial y} = 0 \,, \tag{1}$$

$$\begin{aligned} &\rho_f \left(u\frac{\partial u}{\partial x} + v\frac{\partial u}{\partial y} \right) = \mu \left(1 + \frac{1}{\beta} \right) \frac{\partial^2 u}{\partial y^2} \\ &-\Big\{ (1 - C_\infty)\, \rho_{f_\infty} \left[\beta_T \left(T - T_\infty \right) + \beta_{c_1} \left(C_1 - C_{1\infty} \right) + \beta_{c_2} \left(C_2 - C_{2\infty} \right) \right] \\ &- \left(\rho_p - \rho_{f_\infty} \right) \left(C - C_\infty \right) \Big\} g \,, \end{aligned} \tag{2}$$

$$\begin{aligned} u\frac{\partial T}{\partial x} + v\frac{\partial T}{\partial y} = \alpha\frac{\partial^2 T}{\partial y^2} + \tau \left[D_B \frac{\partial T}{\partial y}\frac{\partial C}{\partial y} + \frac{D_T}{T_\infty}\left(\frac{\partial T}{\partial y} \right)^2 \right] \\ - \frac{1}{(\rho c)_f}\frac{\partial q_r}{\partial y} + D_{TC_1}\frac{\partial^2 C_1}{\partial y^2} + D_{TC_2}\frac{\partial^2 C_2}{\partial y^2} \,, \end{aligned} \tag{3}$$

www.czasopisma.pan.pl PAN POLSKA AKADEMIA NAUK www.journals.pan.pl

$$u\frac{\partial C_1}{\partial x}+v\frac{\partial C_1}{\partial y}=D_{s_1}\frac{\partial^2 C_1}{\partial y^2}+D_{C_1T}\frac{\partial^2 T}{\partial y^2}\,, \tag{4}$$

$$u\frac{\partial C_2}{\partial x}+v\frac{\partial C_2}{\partial y}=D_{s_2}\frac{\partial^2 C_2}{\partial y^2}+D_{C_2T}\frac{\partial^2 T}{\partial y^2}\,, \tag{5}$$

$$u\frac{\partial C}{\partial x}+v\frac{\partial C}{\partial y}=D_B\frac{\partial^2 C}{\partial y^2}+\frac{D_T}{T_\infty}\frac{\partial^2 T}{\partial y^2}\,, \tag{6}$$

where u and v are the velocity components along the x- and y-direction respectively, μ is the coefficient of fluid viscosity, ρ_f is the fluid density, g is the gravitational acceleration, β_T is the volumetric thermal expansion coefficient, β_{c_1} and β_{c_2} are the volumetric solutal expansion coefficient of salt 1 and 2 respectively, ρ_p is the density of the particles, T is the temperature of the fluid, C_1 and C_2 are the solutal concentration of salt 1 and 2 respectively, C is the nanoparticle concentration, $\alpha=k/(\rho c)_f$ is the thermal diffusivity of the fluid, k is the thermal conductivity, c_f and c_p are the specific heat coefficient of fluid and nanoparticle respectively, $\tau=\frac{(\rho c)_p}{(\rho c)_f}$ is the ratio of effective heat capacity of the nanoparticle material to heat capacity of the fluid, q_r is the radiative heat flux, D_B is the Brownian diffusion coefficient, D_T is the thermophoretic diffusion coefficient, D_{TC} and D_{CT} are the Dufour and Soret type diffiusivity, D_S is the solutal diffiusivity.

The boundary conditions for the present flow analysis are:

$$u=0\,,\quad v=0\,,\ T=T_w\,,\ C_1=C_{1w}\,,\ C_2=C_{2w}\,,\ C=C_w\quad\text{at}\ \ \eta=0\,, \tag{7}$$

$$u,\ v\to 0\,,\ T\to T_\infty\,,\ C_1\to C_{1\infty}\ C_2\to\ C_{2\infty}\ C\to C_\infty\quad\text{as}\ \ \eta\to\infty\,. \tag{8}$$

By using the Rosseland approximation, the radiative heat flux, q_r, is given by

$$q_r=\ -\frac{4\sigma^*}{3k^*}\frac{\partial T^4}{\partial y}=-\frac{16\sigma^*}{3k^*}T^3\frac{dT}{dy}\,, \tag{9}$$

where σ^* is the Stefan-Boltzmann constant and k^* is the mean absorption coefficient.

In view to Eq. (9) and Eq. (3) reduces to

$$\begin{aligned}u\frac{\partial T}{\partial x}+v\frac{\partial T}{\partial y}&=\frac{\partial}{\partial y}\left[\left(\alpha+\frac{16\sigma^*T^3}{3k^*(\rho c)_f}\right)\frac{\partial T}{\partial y}\right]\\&+\tau\left[D_B\frac{\partial T}{\partial y}\frac{\partial C}{\partial y}+\frac{D_T}{T_\infty}\left(\frac{\partial T}{\partial y}\right)^2\right]+D_{TC_1}\frac{\partial^2 C_1}{\partial y^2}+\frac{\partial^2 C_2}{\partial y^2}\,.\end{aligned} \tag{10}$$

www.czasopisma.pan.pl PAN POLSKA AKADEMIA NAUK www.journals.pan.pl

Introduce the non-dimensional similarity variables as

$$\psi{=}\alpha \mathrm{Ra}_x^{\frac{1}{4}} f, \quad \mathrm{Ra}_x = \frac{(1-C_\infty)\,\beta_g\,(T_w - T_\infty)\,x^3}{v\alpha}\,, \quad \eta = \mathrm{Ra}_x^{\frac{1}{4}}\frac{y}{x}, \quad u = \frac{\partial \psi}{\partial y},$$

$$v = -\frac{\partial \psi}{\partial x}, \quad T = T_\infty[1 + (\theta_w - 1)\theta\,(\eta)\,], \quad \chi_1\,(\eta) = \frac{C_1 - C_{1\infty}}{C_{1w} - C_{1\infty}}\,,$$

$$\chi_2\,(\eta) = \frac{C_2 - C_{2\infty}}{C_{2w} - C_{2\infty}}, \quad \phi\,(\eta) = \frac{C - C_\infty}{C_w - C_\infty}, \tag{11}$$

where $\theta_w = \frac{T_w}{T_\infty}$, $\theta_w > 1$ being the temperature ratio parameter.

Using Eq. (11), Eq. (1) is automatically satisfied and the nonlinear partial differential Eqs. (2)–(6) are reduced into nonlinear ordinary differential equations as:

$$\left(1 + \frac{1}{\beta}\right) f''' + \frac{1}{4\mathrm{Pr}}\left(3ff'' - 2f'^2\right) - (\theta + Nc_1\chi_1 + Nc_2\chi_2 - Nr\phi) = 0\,, \tag{12}$$

$$\left\{[1 + Rd(1 + (\theta_w - 1)\,\theta)^3]\theta'\right\}' + \frac{3}{4}\theta' f + N_b\theta'\varphi' + N_t\theta'^2 + Nd_1\chi''_1 + Nd_2\chi''_2 + 3Rd[1 + (\theta_w - 1)\theta]^2\,(\theta_w - 1)\,\theta'^2 = 0\,, \tag{13}$$

$$\chi''_1 + \frac{3}{4}\mathrm{Le}_1 f\chi'_1 + Ld_1\theta'' = 0\,, \tag{14}$$

$$\chi''_2 + \frac{3}{4}\mathrm{Le}_2 f\chi'_2 + Ld_2\theta'' = 0\,, \tag{15}$$

$$\phi'' + \frac{3}{4}\mathrm{Le} f\phi' + \frac{N_t}{N_b}\theta'' = 0. \tag{16}$$

Corresponding boundary conditions are,

$$\begin{aligned} &f = 0, \quad f' = 0, \quad \theta = 1, \quad \chi_1 = 1, \quad \chi_2 = 1, \quad \phi = 1 \quad \text{at} \quad \eta = 0 \\ &f' \to 0, \quad \theta \to 0, \quad \chi_1 \to 0, \quad \chi_2 \to 0, \quad \phi \to 0 \quad \text{as} \quad \eta \to \infty \end{aligned} \tag{17}$$

where Nc_1 and Nc_2 are the buoyancy ratios of salt 1 and salt 2, respectively, Nr is the nanofluid buoyancy ratio parameter, Pr is the Prandtl number, N_b is the Brownian motion parameter, N_t is the thermophoresis parameter, Rd is the radiation parameter, Nd_1 and Nd_2 are the modified Dufour parameter of salt 1 and salt 2 respectively, Le_1 and Le_2 are the regular Lewis number of salt 1 and salt 2, nanofluid Lewis number, Le is

www.czasopisma.pan.pl PAN POLSKA AKADEMIA NAUK www.journals.pan.pl

the nanofluid Lewis number, Ld_1 and Ld_2 are the Dufour solutal Lewis number of salt 1 and salt 2.
These parameters are defined as follows:

$$\mathrm{Pr} = \frac{\nu}{\alpha}\,, \quad Nc_1 = \frac{\beta_{C_1}\left(C_{1w} - C_{1\infty}\right)}{\beta_T\left(T_w - T_\infty\right)}\,, \quad Nc_2 = \frac{\beta_{C_2}\left(C_{2w} - C_{2\infty}\right)}{\beta_T\left(T_w - T_\infty\right)}\,,$$

$$Nr = \frac{\left(\rho_p - \rho_{f_\infty}\right)C_\infty}{\left(1 - C_\infty\right)\rho_{f_\infty}\beta_T\left(T_w - T_\infty\right)},\ N_b = \frac{\tau D_B C_\infty}{\alpha},\ \ N_t = \frac{\tau D_T\left(T_w - T_\infty\right)}{\alpha T_\infty},$$

$$Nd_1 = \frac{D_{TC_1}}{\alpha}\frac{\left(C_{1w} - C_{1\infty}\right)}{\left(T_w - T_\infty\right)},\ \ Nd_2 = \frac{D_{TC_2}}{\alpha}\frac{\left(C_{2w} - C_{2\infty}\right)}{\left(T_w - T_\infty\right)},\ \ Rd = \frac{16\sigma^* T_\infty^3}{3kk^*},$$

$$\mathrm{Le}_1 = \frac{\alpha}{D_{S_1}}\,, \quad \mathrm{Le}_2 = \frac{\alpha}{D_{S_2}}\,, \quad Ld_1 = \frac{D_{C_1T}}{D_{S_1}}\frac{\left(T_w - T_\infty\right)}{\left(C_{1w} - C_{1\infty}\right)},$$

$$Ld_2 = \frac{D_{C_2T}}{D_{S_2}}\frac{\left(T_w - T_\infty\right)}{\left(C_{2w} - C_{2\infty}\right)}\,, \quad \mathrm{Le} = \frac{\alpha}{D_B}\,.$$

The local Nusselt number Nu_x and Sherwood number Sh_x^1, Sh_x^2 are defined as follows:

$$\mathrm{Nu}_x = \frac{x}{k\left(T_w - T_\infty\right)}\left(-k\frac{\partial T}{\partial y} + \left(q_r\right)_w\right)_{y=0},\ \ \mathrm{Sh}_x^1 = -\frac{x}{\left(C_{1w} - C_{1\infty}\right)}\left(\frac{\partial C_1}{\partial y}\right)_{y=0},$$

$$\mathrm{Sh}_x^2 = -\frac{x}{\left(C_{1w} - C_{1\infty}\right)}\left(\frac{\partial C_1}{\partial y}\right)_{y=0}. \tag{18}$$

Using Eqs. (9), (11), and (18) is reduced as

$$\left(\mathrm{Ra}_x\right)^{-\frac{1}{4}}\mathrm{Nu}_x = -\left(1 + Rd\ \theta_w^3\right)\theta'\left(0\right), \quad \left(\mathrm{Ra}_x\right)^{-\frac{1}{4}}\mathrm{Sh}_x^1 = -\chi_1'\left(0\right),$$

$$\left(\mathrm{Ra}_x\right)^{-\frac{1}{4}}\mathrm{Sh}_x^2 = -\chi_2'\left(0\right), \tag{19}$$

where $\mathrm{Ra}_x = Ax^3$.

3 Numerical method

The reduced flow governing coupled ordinary differential equations (12)–(16) along with the boundary limitations (17) are resolved numerically using Runge-Kutta based procedure along with shooting method. Initially, the

www.czasopisma.pan.pl PAN POLSKA AKADEMIA NAUK www.journals.pan.pl

set of coupled nonlinear ordinary differential equations (12)–(16) are converted to a system of first order differential equations using the following procedure:

$$f = y_1, \quad f' = y_2, \quad f'' = y_3, \quad \theta = y_4, \quad \theta' = y_5,$$

$$\chi_1 = y_6, \quad \chi_1' = y_7, \quad \chi_2 = y_8, \quad \chi_2' = y_9, \quad \phi = y_{10}, \quad \phi' = y_{11},$$

then

$$y_3' = \frac{1}{\left(1+\frac{1}{\beta}\right)}\left[-\frac{1}{4\mathrm{Pr}}\left(3y_1y_3 - 2y_2^2\right) + \left(y_4 + Nc_1y_6 + Nc_2y_8 - Nry_{10}\right)\right], \tag{20}$$

$$y_5' = \frac{1}{\left[1 + Nd_1Ld_1 + Nd_2Ld_2 + Rd(1+(\theta_w-1)\,y_4)^3\right]} \times \times \begin{bmatrix} -\frac{3}{4}y_1y_5 - Nby_5y_{11} - Nty_5^2 \\ +\frac{3}{4}Nd_1\mathrm{Le}_1y_1y_7 + \frac{3}{4}Nd_2\mathrm{Le}_2y_1y_9 \\ -3Rd(1+(\theta_w-1)\,y_4)^2\,(\theta_w-1)\,y_5^2 \end{bmatrix}, \tag{21}$$

$$y_7' = -\frac{3}{4}\mathrm{Le}_1y_1y_7 + Ld_1y_5', \tag{22}$$

$$y_9' = -\frac{3}{4}\mathrm{Le}_2y_1y_9 + Ld_2y_5', \tag{23}$$

$$y_{11}' = -\frac{3}{4}\,Lny_1y_{11} + \frac{Nt}{Nb}y_5', \tag{24}$$

and the corresponding boundary conditions will becomes:

$$\begin{aligned} y_1 = 0,\ \ y_2 = 0,\ \ y_4 = 1,\ \ y_6 = 1,\ \ y_8 = 1,\ \ y_{10} = 1 \quad \text{at}\ \ \eta = 0, \\ y_2 = 0,\ \ y_4 = 0,\ \ y_6 = 0,\ \ y_8 = 0,\ \ y_{10} = 0 \quad \text{as}\ \ \eta \to \infty. \end{aligned} \tag{25}$$

To solve Eqs. (20)–(25), choose the values of y_3, y_5, y_7, $y_{9.}$, and y_{11} which are not given in the initial conditions. Once all initial conditions are found, then Eqs. (20)–(24) along with (25) are solved through Runge-Kutta Fehlberg fourth-fifth order method with the successive iterative step length of 0.01. The CPU running-time for existing numerical solution was 0.032 s.

www.czasopisma.pan.pl PAN POLSKA AKADEMIA NAUK www.journals.pan.pl

4 Results and discussion

Numerical computations are carried out for several set of values of the buoyancy ratios of salt 1 (Nc_1) and salt 2 (Nc_2), nanofluid buoyancy ratio parameter (Nr), radiation parameter (Rd), Brownian motion parameter (Nb), thermophoresis parameter (Nt), temperature ratio parameter (θ_w), modified Dufour parameter of salt 1 (Nd_1) and salt 2 (Nd_2), regular Lewis number of salt 1 (Le_1) and salt 2 (Le_2), Dufour solutal Lewis number of salt 1 (Ld_1) and salt 2 (Ld_2). In order to analyze the salient features of the problem, the numerical results are presented in Figs. 1–16 and are discussed in detail. Moreover, graphical representations are made for the two cases, i.e., for $\beta = 2$ represents the Casson fluid whereas $\beta = \infty$ refers to viscous fluid.

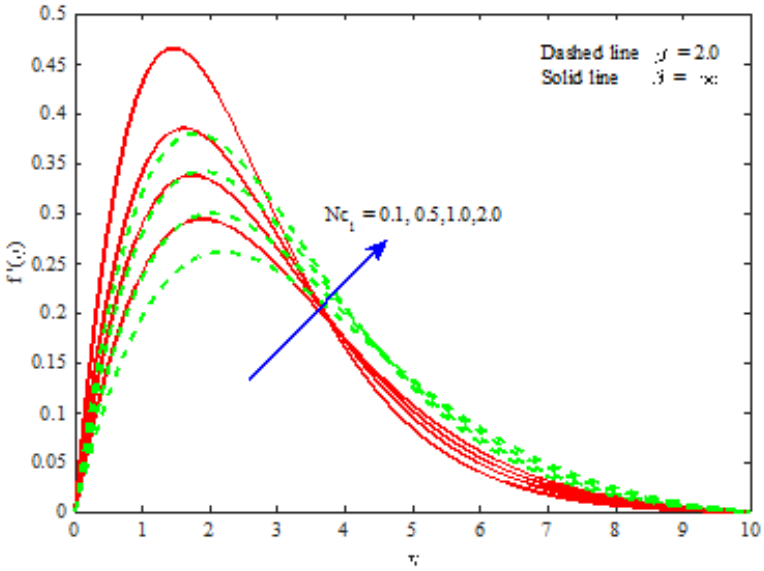

Figure 1: Variation of $f'(\eta)$ for the parameter Nc_1.

Figure 1 and 2 displays the variations in the curves of $f'(\eta)$ corresponding to distinct values buoyancy ratio (Nc_1 and Nc_2.), which is the ratio of fluid density contributions by the two solutes. From the output of these figures it can be perceived that, $f'(\eta)$ for both the salts are much influenced by buoyancy ratio. The reason for this behavior is buoyancy force which dominates with in the boundary layer. But opposite behavior can be seen

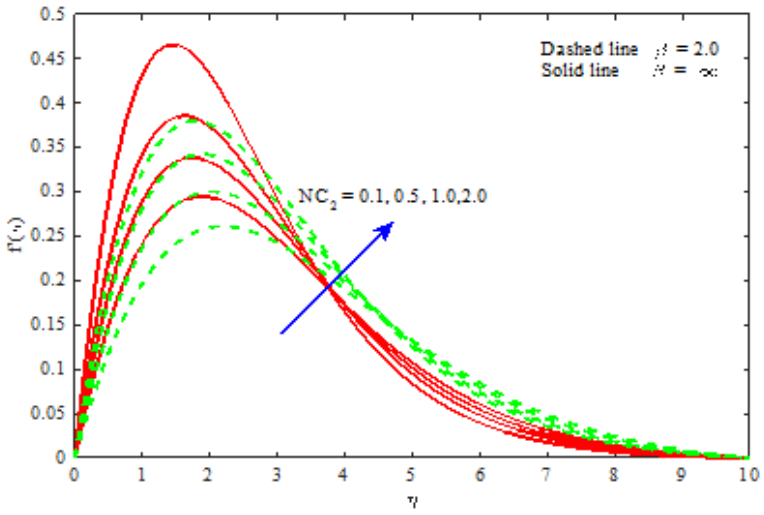

Figure 2: Variation of $f'(\eta)$ on Nc_2.

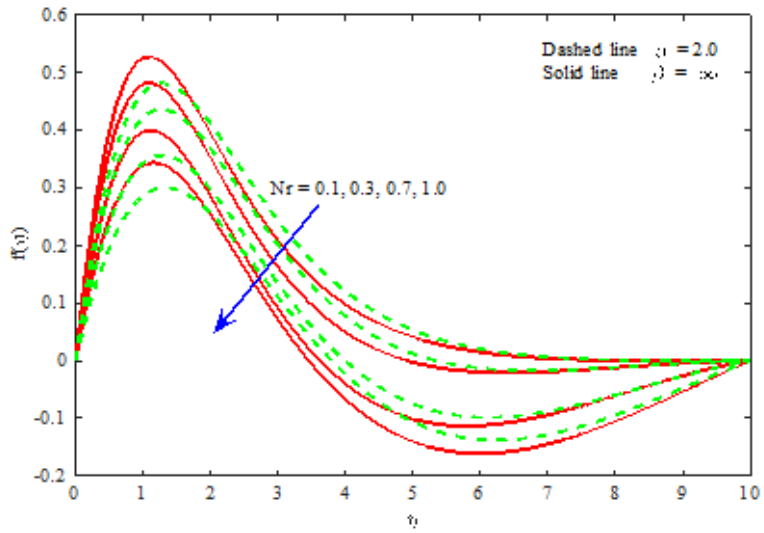

Figure 3: Variation of $f'(\eta)$ on Nr.

for increasing values of Nr which can be viewed from Fig. 3.

Figure 4 exhibits the variation of temperature profile for the radiation parameter. As, the radiation parameter releases the heat energy into the

www.czasopisma.pan.pl PAN POLSKA AKADEMIA NAUK www.journals.pan.pl

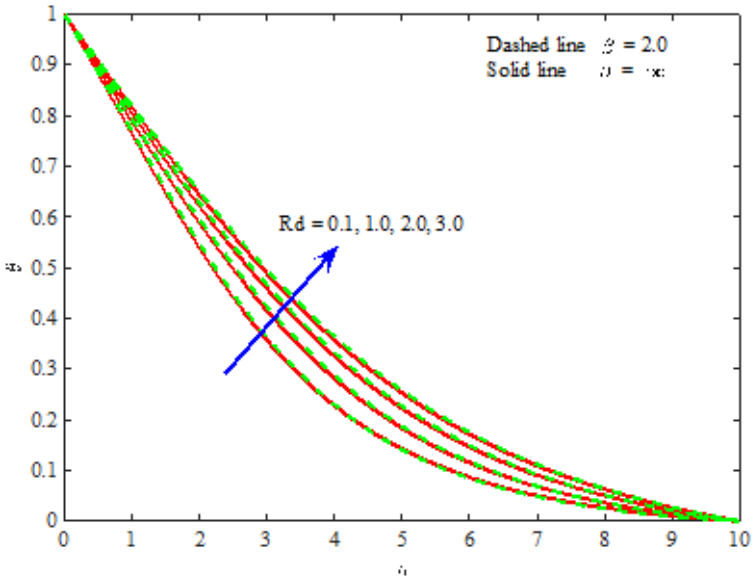

Figure 4: Variation of $\theta(\eta)$ on Rd.

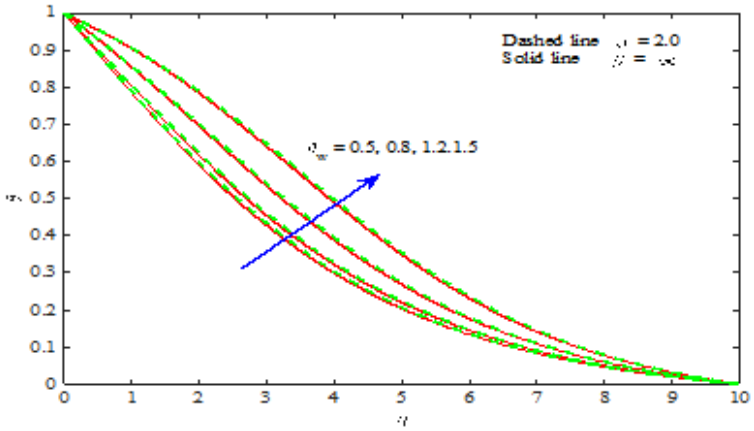

Figure 5: Variation of $\theta(\eta)$ on θ_w.

flow, internal conductivity of the fluid directs the fluid flow to be hotter hence with an increase of radiation parameter, temperature profile increases.

Figure 5 portraits that, the temperature profile is an increasing function of temperature ratio parameter. This phenomenon occurs because,

www.czasopisma.pan.pl PAN POLSKA AKADEMIA NAUK www.journals.pan.pl

temperature ratio parameter describes the thermal state of the fluid and with the increase of this parameter temperature also increases. The role of Brownian motion and thermophoresis parameter on temperature profile can be visualized through Figs. 6 and 7, respectively.

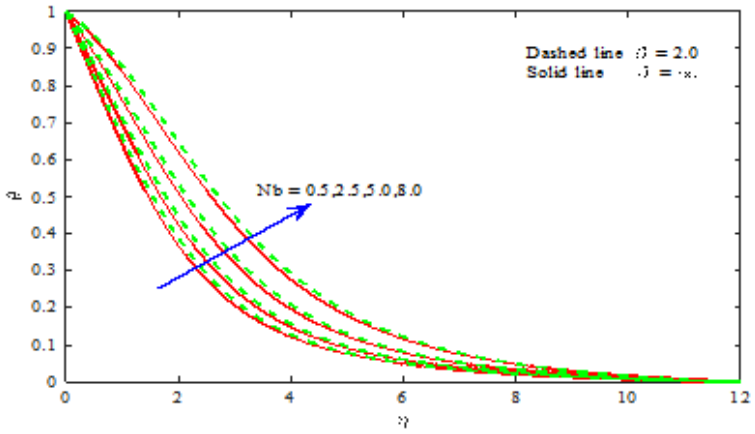

Figure 6: Variation of $\theta(\eta)$ on Nb.

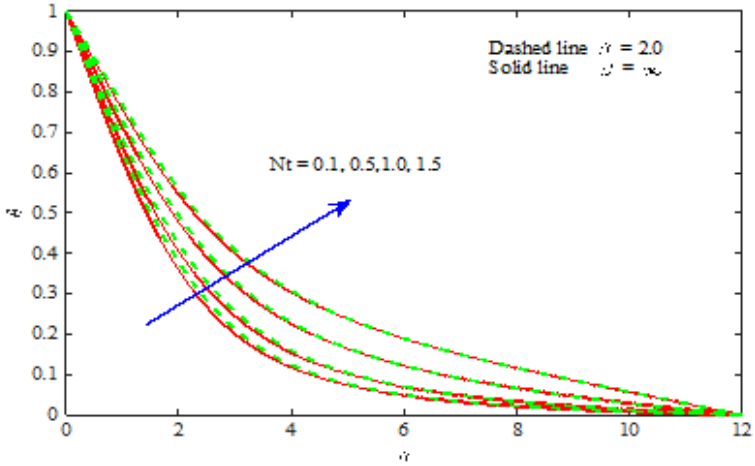

Figure 7: Variation of $\theta(\eta)$ on Nt.

Increase of Brownian motion parameter increases the arbitrary motion of the nanoparticle which causes more heat in the fluid and this leads to increase in temperature of the fluid. Moreover, these two parameters represent the presence of nanoparticle in the fluid. As these particles enhance the thermal conductivity of the fluid, it leads to higher temperature and

www.czasopisma.pan.pl PAN POLSKA AKADEMIA NAUK www.journals.pan.pl

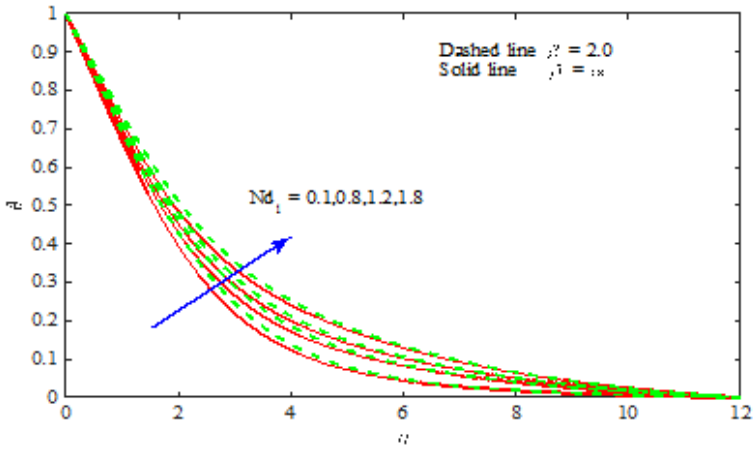

Figure 8: Variation of $\theta(\eta)$ on Nd_1.

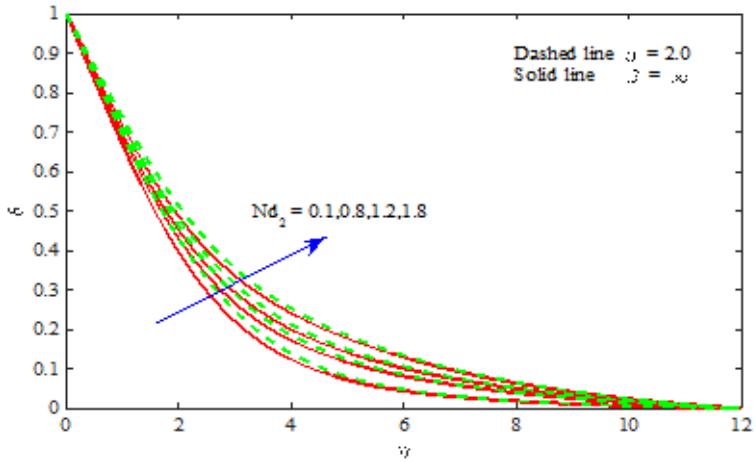

Figure 9: Variation of $\theta(\eta)$ on Nd_2.

thicker thermal boundary layer.

Figure 8 and 9 reveals the impact of modified Dufour parameter of salt 1 and salt 2, respectively, on temperature profile. It is noticed that, temperature profile increases for the larger varying values of modified Dufour parameter. Larger values this parameter leads to increase the temperature as a result of greater thermal diffusivity. As thermal diffusivity increases, thermal conductivity rises which leads to increase in molecular vibrations as a result, temperature increases.

www.czasopisma.pan.pl PAN POLSKA AKADEMIA NAUK www.journals.pan.pl

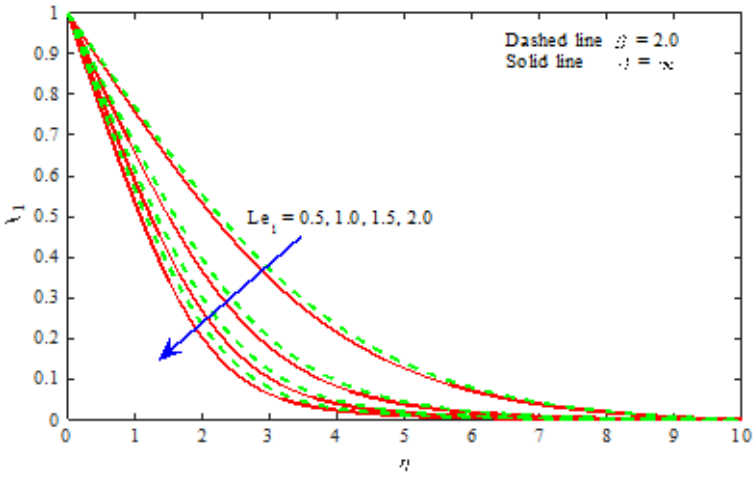

Figure 10: Variation of $\chi_1(\eta)$ on Le_1.

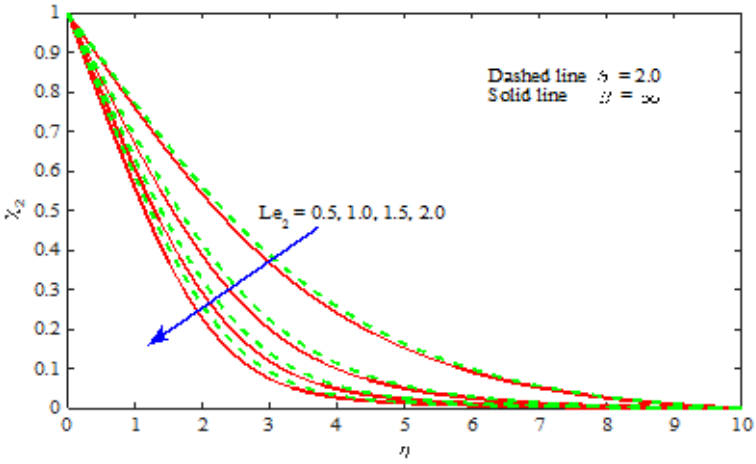

Figure 11: Variation of $\chi_2(\eta)$ on Le_2.

Effect of regular Lewis number for salt 1 and salt 2 on solutal concentration profiles 1 and 2 are analyzed in Figs. 10 and 11, respectively. It emphasizes that, an increase of this number makes the profile to degrade due to the dependency of number on diffusion of solutal coefficient.

The variation of solutal concentration profiles 1 and 2 for Dufour solutal Lewis number of salt 1 and salt 2 are plotted in Fig. 12 and 13, respectively. A significant increase of solutal concentration profile can be seen for these parameters as a result of greater mass diffusivity. Higher mass

www.czasopisma.pan.pl PAN POLSKA AKADEMIA NAUK www.journals.pan.pl

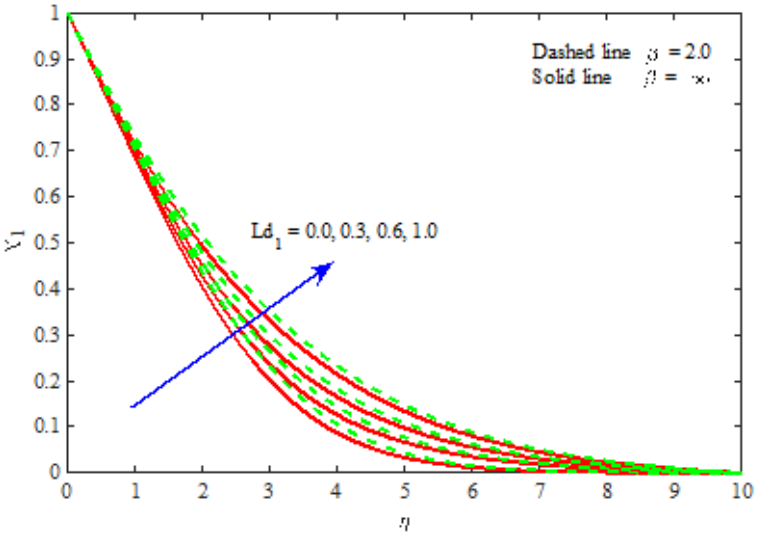

Figure 12: Variation of $\chi_1(\eta)$ on Ld_1.

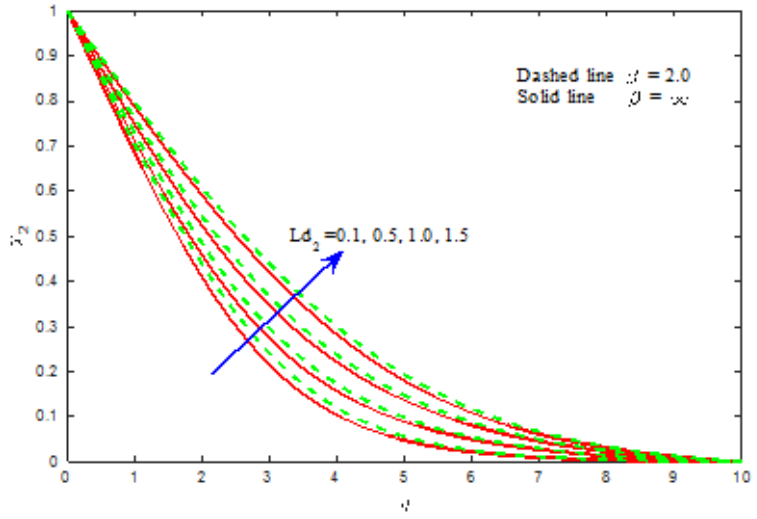

Figure 13: Variation of $\chi_2(\eta)$ on Ld_2.

diffusivity represents greater probability of molecular collision which is the result of large difference in solutal concentration. Higher the concentration gradient increases the difference in solutal concentration of molecules. It

www.czasopisma.pan.pl PAN POLSKA AKADEMIA NAUK www.journals.pan.pl

can be inferred that increase in mass diffusivity increases solutal concentration gradient resulting in solutal increased concentration and thickens the corresponding boundary layer. Moreover, it is noticed that the solutal concentration decreases exponentially from its maximum value at the plate to its minimum value at the end of the boundary layer.

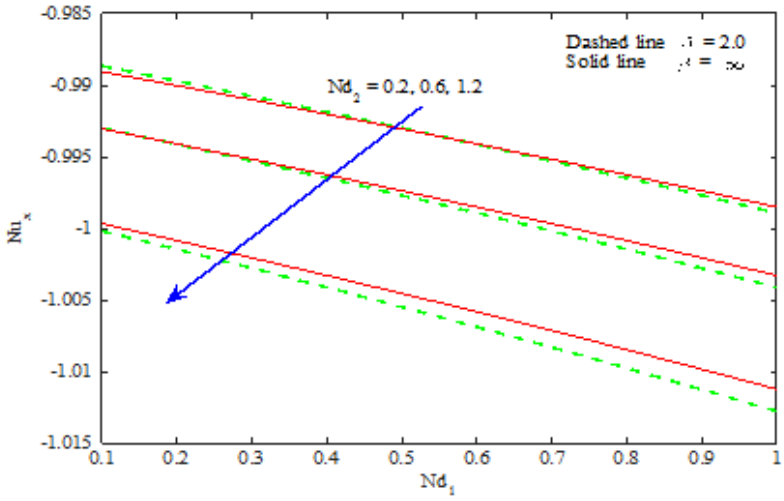

Figure 14: Variation of Nu_x for Nd_1versus Nd_2.

Nusselt number for Nd_1, versus Nd_2 gradually decreases and it is illustrated in Fig. 14. From Figs. 15 and 16, it is clearly observed that Sherwood number increases for the parameter Le_1 versus Ld_1 and Le_2 versus Ld_2. Further from these figures it is noted that, variation of Sherwood number can be seen appropriately faraway from the boundary.

www.czasopisma.pan.pl PAN POLSKA AKADEMIA NAUK www.journals.pan.pl

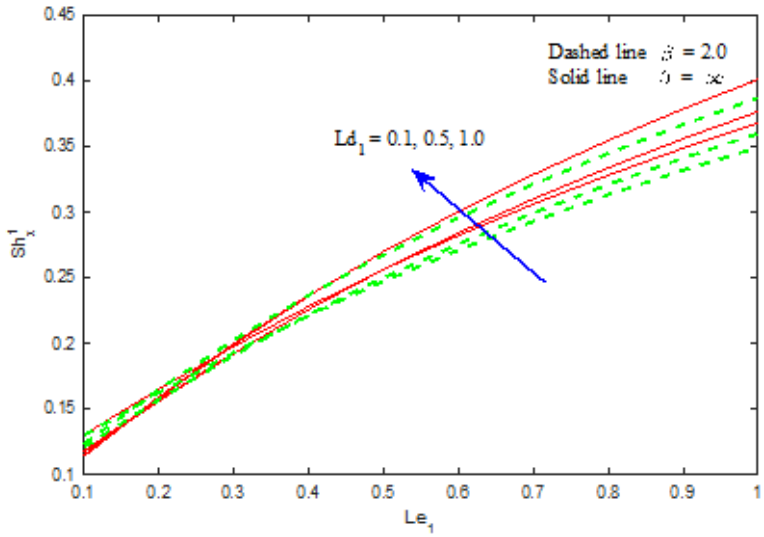

Figure 15: Variation of Sh_x^1 for Le_1 versus Ld_1.

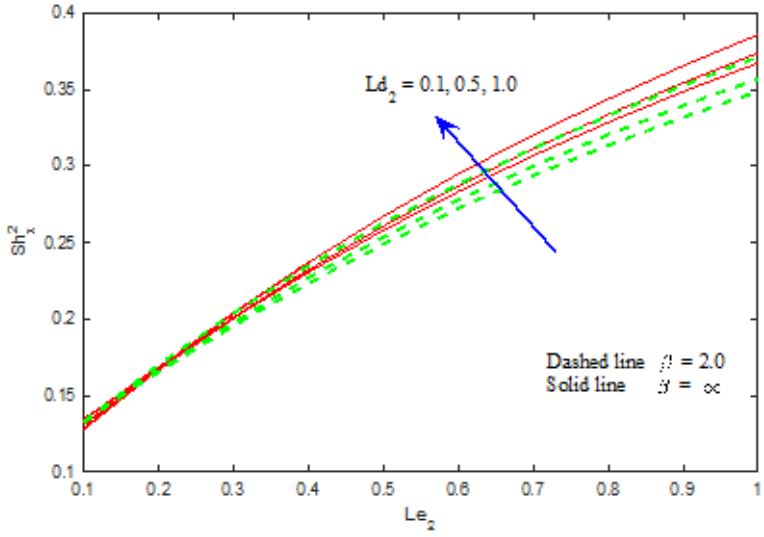

Figure 16: Variation of Sh_x^2 for Le_2 versus Ld_2.

5 Conclusion

Triple diffusive boundary layer flow of Casson nanofluid is scrutinized in the presence of nonlinear thermal radiation. The impact of various physical

www.czasopisma.pan.pl PAN POLSKA AKADEMIA NAUK www.journals.pan.pl

parameters are reviewed for different profiles and corresponding results are summarized as follows:

1. Velocity profile decreases for larger values of nanofluid buoyancy ratio parameter.
2. Thermal boundary layer is thicker for the effect of Brownian motion parameter, thermophoresis parameter, radiation parameter, temperature ratio parameter, modified Dufour parameter.
3. For regular Lewis number of salt 1 and 2, solutal 1 and solutal 2 profiles decreases respectively. Further same behaviour can be seen for Dufour solutal Lewis number for the corresponding profiles.
4. As compared to viscous fluid, temperature component enhances more for the Casson fluid.

Received 8 July, 2017

References

[1] Griffiths R.W.: *The influence of a third diffusing component upon the onset of convection*. J. Fluid Mech. **92**(1979), 4, 659–670.

[2] Kuznetsov A.V., Nield D.A.: *Double-diffusive natural convective boundary-layer flow of a nanofluid past a vertical plate*. Int. J. Therm. Sci. **50**(2011), 5, 712–717.

[3] Rionero S.: *Triple diffusive convection in porous media*. Acta Mech. **224**(2013), 2, 447–458.

[4] Shivakumara I.S., Naveen Kumar S.B.: *Linear and weakly nonlinear triple diffusive convection in a couple stress fluid layer*. Int. J. Heat Mass Tran. **68**(2014), 542–553.

[5] Khan W.A., Culham J.R., Khan Z.H., Pop I.: *Triple diffusion along a horizontal plate in a porous medium with convective boundary condition*. Int. J. Therm. Sci. **86**(2014), 60–67.

[6] Ghalambaz M., Moattar F., Karbassi A., Sheremet M.A., Pop I.: *Triple-diffusive mixed convection in a porous open cavity*. Transp. Porous Med. **116**(2017), 2, 473–491.

[7] Choi S.U.S.: *Enhancing thermal conductivity of fluids with nanoparticles*. In: Proc. ASME Int. Mechanical Engineering Congress and Exposition **66**(1995), 99–105.

[8] Gorla R.S.R., Chamkha A.: *Natural convective boundary layer flow over a horizontal plate embedded in a porous medium saturated with a nanofluid*. J. Modern Physics **2**(2011), 2, 62–71.

www.czasopisma.pan.pl PAN POLSKA AKADEMIA NAUK www.journals.pan.pl

[9] Shehzad S.A., Abbasi F.M., Hayat T., Alsaedi F.: *MHD mixed convective peristaltic motion of nanofluid with Joule heating and Thermophoresis effects.* PLOS One **9**(2014), 11, e111417 1-16.

[10] Sheikholeslami M., Rashidi M.M., Hayat T., Ganji D.D.: *Free convection of magnetic nanofluid considering MFD viscosity effect.* J. Mol. Liq. **218**(2016), 393–399.

[11] Hayat T., Khan M.I., Waqas M., Alsaedi A., Khan M.I.: *Radiative flow of micropolar nanofluid accounting thermophoresis and Brownian moment.* Int. J. Hydrogen Energ. **42**(2017), 26, 16821–16833.

[12] Archana M., Gireesha B.J., Rashidi M.M., Prasannakumara B.C., Gorla R.S.R: *Bidirectionally stretched flow of Jeffrey liquid with nanoparticles, Rosseland radiation and variable thermal conductivity.* Arch. Thermodyn. **39**(2018), 4, 33–57.

[13] Rana G.C., Chand R., Sharma V., Sharda A.: *On the onset of triple-diffusive convection in a layer of nanofluid.* JCAMECH **47**(2016), 1, 67–77.

[14] Goyal R., Bhargava R.: *FEM simulation of triple diffusive magnetohydrodynamics effect of nanofluid flow over a nonlinear stretching sheet.* Int. J. Mathematical, Computational, Phys. Elec. Comput. Eng. **10**(2016), 9, 416–423.

[15] Khan Z.H., Khan W.A., Pop I.: *Triple diffusive free convection along a horizontal plate in porous media saturated by a nanofluid with convective boundary condition.* Int. J. Heat Mass Tran. **66**(2013), 603–612.

[16] Khan Z.H., Culham J.R., Khan W.A., Pop I.: *Triple convective-diffusion boundary layer along a vertical flat plate ina porous medium saturated by a water-based nanofluid.* Int. J. Therm. Sci. **90** (2015), 53–61.

[17] Casson N.: *A flow equation for pigment oil suspensions of the printing ink type.* In: Rheology of Sisperse Systems (C.C. Mill Ed.) Pergamon Press, Oxford 1959, 84–102.

[18] Hayat T., Shehzad S.A., Alsaedi A.: *Soret and Dufour effects on magnetohydrodynamic (MHD) flow of Casson fluid.* Appl. Math. Mech. -Engl. Ed. **33**(2012), 10, 1301–1312.

[19] Mabood F., Abdel-Rahman R.G., Lorenzini G.: *Effect of melting heat transfer and thermal radiation on Casson fluid flow in porous medium over moving surface with magnetohydrodynamics.* J. Eng. Thermophys. **25**(2016), 4, 1–12.

[20] Ramesh G.K., Prasannakumara B.C. ,Gireesha B.J., M.M.Rashidi: *Casson fluid flow near the stagnation point over a stretching sheet with variable thickness and radiation.* J. Appl. Fluid Mech. **9**(2016), 3, 1115–1122.

[21] Ibrahim W., Makinde O.D.: *Magnetohydrodynamic stagnation point flow and heat transfer of Casson nanofluid past a stretching sheet with slip and convective boundary condition.* J. Aerospace Eng. **29** (2016), 2, 04015037 1–11.

[22] Waqas M., Farooq M., Khan M.I., Alsaedi A., Hayat T., Yasmeen T.: *Magnetohydrodynamic (MHD) mixed convection flow of micropolar liquid due to nonlinear stretched sheet with convective condition.* Int. J. Heat . Mass Tran. **102**(2016), 766–772.

www.czasopisma.pan.pl PAN POLSKA AKADEMIA NAUK www.journals.pan.pl

[23] Hayat T., Khan M.I., Farooq M., Yasmeen T., Alsaedi A.: *Stagnation point flow with Cattaneo-Christov heat flux and homogeneous-heterogeneous reactions*. J. Mol. Liq. **220**(2016), 49–55.

[24] Khan M.I., Waqas M., Hayat T., Alsaedi A.: *A comparative study of Casson fluid with homogeneous-heterogeneous reactions*. J. Colloid Interf. Sci. **498**(2017), 85–90.

[25] Makinde O.D., Animasaun I.L.: *Thermophoresis and Brownian motion effects on MHD bioconvection of nanofluid with nonlinear thermal radiation and quartic chemical reaction past an upper horizontal surface of a paraboloid of revolution*. J. Mol. Liq. **221**(2016), 733–743.

[26] Mustafa M., Mushtaq A., Hayat T., Alsaedi A.: *Rotating flow of magnetite-water nanofluid over a stretching surface inspired by non-linear thermal radiation*. PLOS ONE, 11 (2016), 2, 0149304 1–16.

[27] Archana M., Gireesha B.J., Venkatesh P., Reddy M.G.: *Influence of non-linear thermal radiation and magnetic field on three-dimensional flow of a Maxwell nanofluid*. J. Nanofluids **6**(2017), 2, 232–242.

[28] Ramesh G.K., Prasannakumara B.C., Gireesha B.J., Shehzad S.A., Abbasi F.M.: *Three dimensional flow of Maxwell fluid with suspended nanoparticles past a bidirectional porous stretching surface with thermal radiation*. Therm. Sci. Eng. Prog. **1**(2017), 6–14.

[29] Hussain S.T., Ul Haq R., Noor N.F.M., Nadeem S.: *Non-linear radiation effects in mixed convection stagnation point flow along a vertically stretching surface*. Int. J. Chem. Reactor Eng. **15**(2017), 1 doi.org/10.1515/ijcre-2015-0177.

[30] Farooq M., Khan M.I., Waqas M.,Hayat T., Alsaedi A., Khan M.I.: *MHD stagnation point flow of viscoelastic nanofluid with non-linear radiation effects*. J. Mol. Liq. **221**(2016), 1097–1103.

[31] Khan M.I., Alsaedi A., Shehzad S.A., Hayat T.: *Hydromagnetic nonlinear thermally radiative nanoliquid flow with Newtonian heat and mass conditions*. Results Phys. **7**(2017), 2255–2260.